Identification of environmental buffer areas in urbanized catchments based on synthetic ecosystem functions

Yuliana Céliz[abc1*], Diego Pons[b**], Beatriz Giobellina[bc***], Marcos Zefferino[d****]

[a]*CONICET- Consejo Nacional de Investigaciones Científicas y Técnicas, Argentina*

[b]*Instituto Nacional de Tecnología Agropecuaria –INTA-EEA Manfredi, Ruta Nacional N°9 Km636, Manfredi CP5988, Argentina*

[c]*Observatorio de Agricultura Urbana Periurbana y Agroecología (O-AUPA) AER Córdoba INTA-, Presidente Roca y La Coruña. Córdoba CP5000, Argentina.*

[d]*Universidad Tecnológica. Centro Sur. Área de Energías Renovables. Francisco Antonio Maciel s/n esq. Luis Morquio. Durazno CP97000 Uruguay.*

Keywords: Land-use planning; ecosystem services; hydrological index; natural area; urban areas.

Abstract

The Saldán river basin in the northwest of the metropolitan area of Córdoba, Argentina, was defined as a unit for the observation of ecosystem services of water regulation. The capacity of the system to retain excess rainfall through vegetation in areas with slopes was analyzed. The observation area was a wildland-urban interface. From there, a model capable of synthesizing the behavior of the most relevant variables in the event of an extraordinary rainfall event was adjusted. The result was the definition of buffer areas or ecosystemic protection in the interface. The testing and adjustment of this model defined a REP indicator that was proposed as an input in the planning of the sector. For validation, soil moisture permanence values from LWI were used. The derivative was calculated for each pixel value in the basin, for both dry and wet periods, and the areas with the lowest loss in both periods were compared with those with the highest retention obtained in the model. The zones identified by both methods show great similarities.

1. Introduction

The expansion of cities, observed as the process of landscape anthropization, implies major impacts on the dynamics of land use. According to World Bank data, 56% of the population lives in cities (WORLD BANK, 2020). In Argentina, this percentage rises to 92%. The speed of the increase in these data shows a clear focus on the growth of the built-up area and the impact this has on ecosystems (Elmqvist et al., 2013).

Urbanization advances on territories whose fundamental ecological processes for sustainability are invisible to planners. Natural and semi-natural areas are anthropized and the consequences are evident when it has direct impacts on the population or the process is

[1*]**Yuliana Céliz.** Address: *Virrey Arredondo 2553. Ciudad Autónoma de Buenos Aires. CP1426- Argentina* Tel.: +543516849466; email: yulianaceliz09@gmail.com. ORCID: https://orcid.org/0000-0003-3810-8490
****Diego Pons**. Address:*Ruta Nacional N°9 Km636, Manfredi CP5988, Argentina.* Tel. +5493515313711. email:pons.diego@inta.gob.ar
*****Beatriz Giobellina.** Address: *Bv. Los Andes 167.Córdoba CP5000- Argentina*. Tel.+5493513171964. email: giobellina.beatriz@inta.gob.ar
******Marcos Zefferino**.Address: Oscar Gestido 2622. Montevideo-CP11300-Uruguay. Tel: +59899963490. email:marcos.zefferino@utec.edu.uy

already irreversible. It follows that the density, spatial distribution and physical characteristics of human settlements are important drivers of social and environmental change at multiple scales (Massey, 2005).

The space where land use and land cover change occurs most intensively is defined as an interface (Céliz, 2020). This area is characterized by the interaction of two or more mutually affected systems, generating a new space with its own characteristics and dynamics. The heterogeneity of this area, as well as the coexistence of natural and urban systems, makes its spatial definition very complex. The speed and effects of these transformations require information that incorporates into land use planning (LUP) processes, the visibility of areas associated with ecological processes that affect human settlements and increase their exposure to risk.

The city of Córdoba is an example of this dynamic scenario, where the urbanized surface area increased from 7700 ha in 1976 to 14400 ha in 2014 (Mari & Pons, 2015). The detection of these changes in land cover determined the urban advance over food-producing areas (Giobellina 2016, Giobellina et al., 2022) in the metropolitan south and, to the northwest, over forest areas (Gavier & Bucher, 2004). In the case of these types of natural areas, the process is associated with an increase in the probability of fires (Argañaraz et al., 2017), greater exposure of human settlements to extraordinary events such as floods (Barbeito, Ambrosino & Rydzewski, 2015; Barchuk, 2016), or erosion (Barbeito et al., 2015), among others.

The point of interest is based on the possibility and effectiveness of spatializing synthetic and useful ecosystemic processes for LUP but, at the same time, the simplification implied by the spatialization of certain processes does not generate false results or results that are too far from reality.

Furthermore, work in the area of natural sciences has been crucial in the possibility of delimiting ecological processes for their quantification, based on methodologies for valuation of ecosystem services. De Groot et al. (2002) propose a classification of ecosystem functions, goods and services in which it is assumed that the main ecosystem services (soil protection, production, purification and supply of water, provision of habitat and shelter) are directly associated with the amount of biomass present in the ecosystem.

Viglizzo and Frank (2006) proposed a methodological framework to evaluate land-use options through tradeoff analysis (ecosystem and economic provisioning of services) in the Argentine pampas. They defined functional complementation of biomes as a smart strategy to explore land-use options on a large scale (regional and temporal). Then, Raudsepp-Hearne et al. (2010) analyzed the provision of multiple ecosystem services in periurban agricultural landscapes, identifying tradeoffs between provisioning and almost all regulation and cultural ecosystem services. This study defined that, an increased diversity of ecosystem services is positively correlated with regulation ecosystem services. Afterwards, Carreño et al. (2012) estimated the regional provision of ecosystem services in Argentina using land-use and vegetation cover registers from 657 administrative districts from the national agricultural census (INDEC, 1964, 1991, 2004) and agricultural surveys (SAGPyA, 2009). Also, adaptations on the models of Carreño et al. were reviewed, implemented by Laterra et al. (2015) and Barral (2017). Most of these authors did not establish a particular consideration regarding the interaction of these processes with the urban variable and the weight that this can have in the models applied in interface areas.

The purpose of this work was to adapt the methodology of spatialization of basic ecosystem processes taking into account the anthropic impact of urbanization. The aim is to establish a

baseline to address strategic lines of protection for areas that perform critical ecosystem functions for socio-ecosystems according to their specific context.

2. Materials and methods

2.1 Study area and conditions

The city of Córdoba is situated in the geographical center of Argentina. Its metropolitan area was established by the provincial Land Use Law (No. 9841) (Arias and Campana, 2012) and has 263.000 hectares. Within this area, Córdoba is the most important city in the province and the second at the national level with 1.370.585 inhabitants (INDEC, 2010).

As observed, in the face of urbanization expansion processes in the metropolitan area of Córdoba (AMC), the environment with the greatest impact due to cover substitution was the natural area (Céliz & Maidana, 2019). This area is mostly conformed in the northwest by native forest, for this reason this environment was selected to analyze ecological processes in this study. Likewise, this dynamic was contrasted by several studies associated with extraordinary precipitations events (Gianre, 2015; Lehmann, 2015) .

Through the analysis of general hydrological processes, the Saldán river catchment was defined as the unit to test the modeling of ecosystem functions (Figure 1). The total area of the basin was estimated at 24,729 hectares. This sector, located in the northwest of the MCA, concentrates the highest percentage of urban development on the previously identified mountain forest.

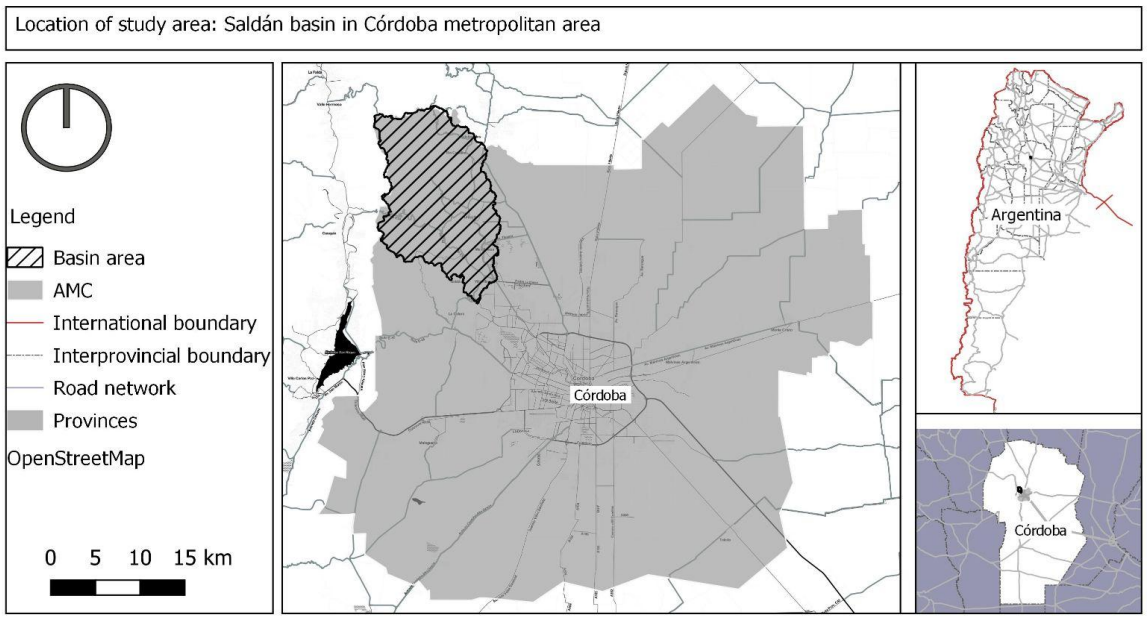

Figure 1. Saldán catchment area

2.2. Identification of ecosystem functions

In general terms, ecosystems play an important role as regulators of the hydrological cycle (Eagleson 2002 cited on Jobbágy (2011)) and in particular, the structure and dynamics of vegetation influence hydrological processes and attributes. According to Jobbágy (2011), the provision and regulation of water flows should be considered when exploring services or synergies with different possible land uses. Also relevant are the attributes of the ecosystem

capable of influencing soil infiltration rates, which are particularly sensitive to interventions including fire and paving due to urbanization, among others (Allan 2004 cited on Jobbágy (2011)). A close link was observed between the occurrence of extraordinary precipitation events and the loss of natural areas due to urbanization (INA-CIRSA, 2004; Ambrosino et al., 2004; Barchuk et al., 2016), so this indicator was taken as the starting point to define areas of maximum ecosystem protection in the basin. The period of analysis selected was January-December 2017 since at the time of this study it was the last year of complete satellite information available.

According to Carreño et al (2012), the capacity of the soil for purification and water supply will depend on its ability to process these water flows entering the system. Therefore, a greater biomass is associated with a greater capacity of the landscape to intercept, retain, and infiltrate water (Postel & Thompson, 2005). This capacity decreases with slope as the time that water remains in the landscape decreases (Carreño & Viglizzo, 2007). Based on the above authors, its proposed the indicator of the water purification and supply capacity of the land (SWPL)(Carreño, Frank & Viglizzo, 2012):

$$SWPL = B \times (1 - VC_B) \times Fsic \times Fpre \times (1 - Fslo)$$

This indicator does not analyze the water needed by the forest ecosystem or what percentage of the total rainfall it incorporates, but it reveals the capacity of the ecosystem to retain excess rainfall during extraordinary events of the regime. Here it is assumed that the capacity of the ecosystem to intercept, retain and infiltrate rainfall depends on the biomass (B) and its stability (VCB), the infiltration capacity of the soil (Fsic), the precipitation (Fpre) and the slope (Fslo).
Adaptations made to this equation for the ECO-SER protocol (Laterra et al.,2015) specify that the ecosystem function of retention of excess rainfall by vegetation cover (REP) is defined as the storm water intercepted by the ecosystem in a year based on the index proposed by Fu et al. (2013) in Barral (2016). Although in this index the most influential parameters are associated with the hydrological calculation for territories without a slope, the annual clipping was taken for the adaptation of the model proposed around the rainfall in the basin. Based on this, the rest of the variables were also calculated for the same year.

2.3. Indicator adaptation to interface areas

To adapt the model equation and define the weight of each variable, biophysical information was obtained from spectral data derived from satellite images from open access libraries and national public databases for local precipitation. In the case of the urban variable, the Normalized Builtup Area Index -NBAI- (Waqar et al., 2012) was calculated and values associated with the waterproofing capacity of the area were obtained as a function of the built-up area. The adapted indicator was defined as follows:

$$REP=(B*(1-CV_B)*Fcis*Fprec*(1-Fpend))*AIUrb$$

Given the normalized difference vegetation index -NDVI-(Tucker, 1979) has shown to have a strong relationship with biomass(Tucker, 1977; Gerberman, Cuellar and Gausman, 1984; Sellers, 1985; Paruelo, 2008), the biomass values (B) for this indicator were obtained from it. The values were derived from a scene of Landsat 8 (21 January 2017). The biomass stability (CV_B) was obtained from the Landsat 8 collection -Collection 1 Tier 1 calibrated

top-of-atmosphere (TOA) reflectance-, available for 2017 through Google Earth Engine (Gorelick *et al.*, 2017). The number of scenes available for that year in the sector was filtered by the presence of clouds. A maximum NDVI value was then obtained for each scene - out of a total of 39 scenes - and the average value per pixel was taken for the basin. The values of both data sets were normalized according to the indicator, in a range of 0-1, where 1 corresponded to the highest NDVI values for the biomass and its stability values.

To determine the infiltration capacity of the soil (Fcis), we used the Soil Chart of the National Institute of Agricultural Technology (Bahill *et al.*, 2015), where the main characteristics of the soil were identified: type, drainage and texture. The values were then normalized to a range of 0 -1, where 1 is the soil with the highest infiltration capacity and 0 the lowest.

For the slope variable (Fpend), a 30m terrain elevation model -SRTM DEM- was used to work with data at the same scale as the Landsat scene information. The information from the DEM was used to generate a slope raster from the SAGA plug-in in QGIS software. Subsequently, slope data were normalized to values between 0 and 1, where the higher altitude areas were considered less able to retain excess precipitation and the lower slope areas -valley areas- were considered able to retain it.

The precipitation variable (Fprec) was elaborated based on data obtained from the website of the Agro-industry National Ministry, from monthly values according to specific geographic coordinates in the study area. In order to have local data and identify spatial variability of rainfall, 20 random points were taken, with information of monthly values. The maximum annual value was obtained for each location and a raster image was constructed using the IDW -inverse distance weighting- interpolation method (Mitas & Mitasova, 1999). Later, they were normalized to values between 0 and 1, where 1 was the area with the highest amount of mm fallen in the year and 0 the one with the lowest.

The waterproofed urbanization area (AIUrb) was calculated based on the NBAI index that uses the relationship between the TM7, TM5 and TM2 bands (Landsat 5) and that were translated according to the bandwidth used to the SWIR2, SWIR1 and GREEN bands respectively in Landsat 8OLI. The patterns identified in the spectral signatures between these band ratios differed from the bare ground, thus reducing the pixel assignment error that is common in the identification of urbanized areas with other indices.

As the process analyzed in this article is the presence and permanence of water in the soil and vegetation, the combination of the GREEN and NIR bands (Landsat 8OLI) was used.which provide the potential to maximize the typical reflectance of water features using the wavelengths of green light, minimizing the NIR response for water features and taking advantage of the high NIR reflectance of vegetation values and soil features. When this relationship is used to process a multispectral image containing a green band in the visible and a NIR band, water features have a positive value, while soil and vegetation features have negative or zero values. This band ratio is defined as NDWI -Normalized difference water index- (Gao, 1996). As this index is derived in the same way as NDVI (Justice et al., 1985) the interpretation of these values is given in a similar way. For example, while NDVI provides an estimate of terrestrial biomass, it cannot provide species discrimination. Thus, an NDWI calculation will not distinguish suspended sediments with chlorophyll, but will provide general information on generic turbidity as analogous to total biomass. This model was run for the catchment area, but the negative corrected values decreased the possibility of spatial comparison. Replacing GREEN with SWIR in this banding relationship has the potential to recover the water content of the canopy (Ceccato et al., 2002). This combination of NIR and SWIR bands (Jürgens, 1997; Xiao, X Boles, S Frolking et al., 2002; Xiao et al., 2004) was defined as the Surface Water Index or LSWI (GAO, 1996; Xiao et al. 2002; 2004,

Chandrasekar et al., 2010).This index was calculated for the same period: January-December 2017 in the catchment area.

For the validation of the REP model, its response was studied according to temporal variations of the main independent variables. In particular, based on the LSWI, the variation of soil moisture presence during a year was observed, differentiating periods of higher and lower annual precipitation. From there, the retention areas of the REP model were evaluated with those of lower moisture loss that identified the temporal variation of LSWI values, and how this variation would indicate areas of retention or no moisture loss in the soil.

LSWI was used as an independent variable or covariate, so that the values obtained could be analyzed using similar methodologies but in isolation. The objective was to obtain soil moisture loss data without resorting to complex procedures (hydrological models or work with radar images) that exceed the scope of this article.

Since in the validation analysis, the condition of soil water permanence or loss has a temporal component, all available scenes for the watershed corresponding to the study year were used. The temporal variation rate of LSWI per pixel was calculated for each available Landsat 8 scene. Once the temporal filters and the presence of clouds were applied, 14 scenes were obtained from which the green and swir bands were selected for LSWI calculation. Subsequently, the mean monthly precipitation values were observed in 3 points of the basin and the scenes were divided into dry and wet periods. From there, the first derivative was calculated for each pair of pixels of each pair of scenes, taking into account the time elapsed between one and the other as follows:

$$\Delta LSWI = \frac{\Delta x}{\Delta t}$$

Where Δx is the difference between two LSWI values for the same pixel in two consecutive scenes and Δt is the time elapsed between these scenes. The mean was then obtained for each period divided into wet period 1 (January-April), dry period (May-September) and wet period 2 (October-December). The pixels that during the 3 calculated periods remained with lower water loss (derivative close to 0) were inferred as those with higher storage or retention capacity. Subsequently, the area of pixels with greater capacity to retain excess precipitation due to vegetation cover was compared with those pixels weighted by the presence of soil moisture obtained from the calculation of the temporal derivative of LSWI.

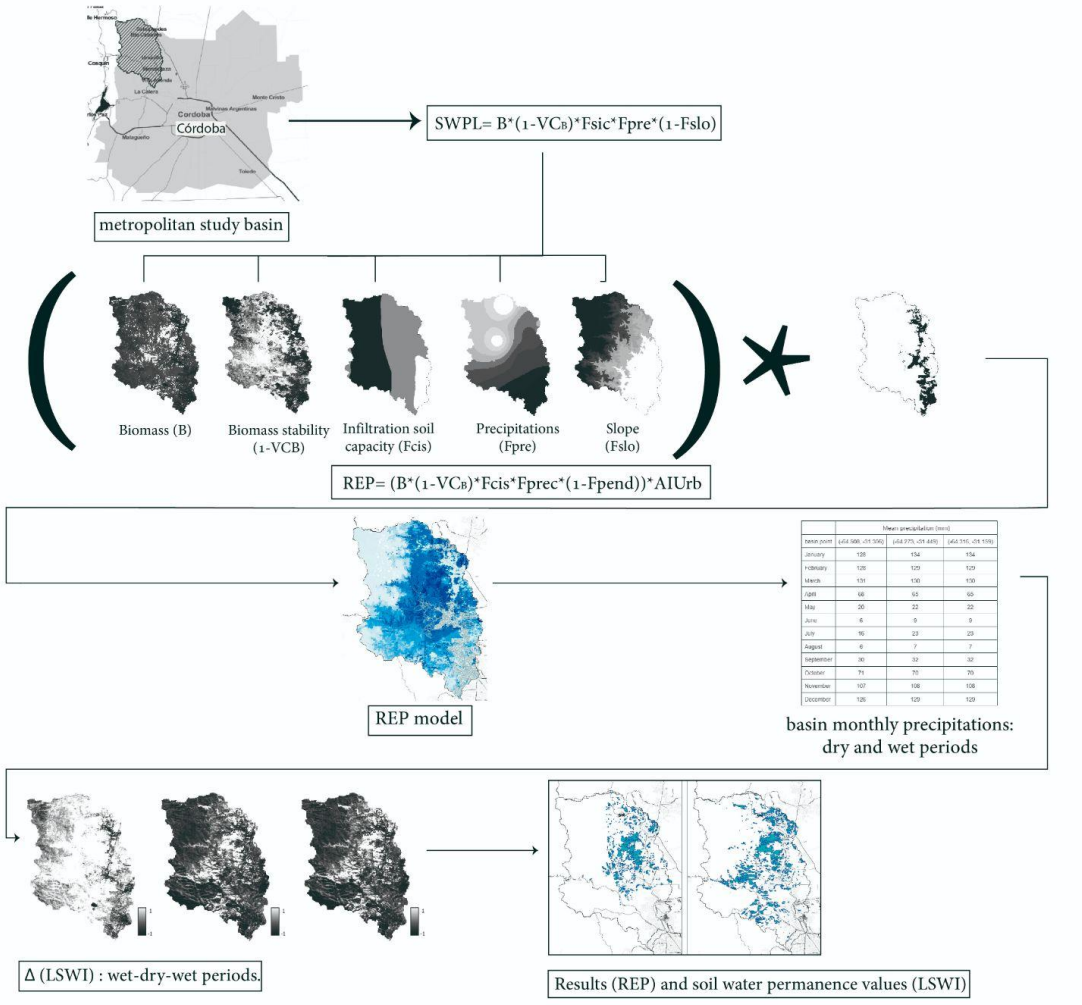

Figure 3. Workflow diagram

3. Results and discussion

3.1 Intermediate products

After observing the environments most affected by anthropization, the retention rate of excess precipitation by vegetation cover (REP) was tested. Intermediate products were obtained for 2017 (Figure 4) these was associated with biophysical processes involved and the urbanized area: biomass (B), biomass stability (CV_B), soil infiltration capacity (Fcis), maximum annual rainfall (Fprec), slope (Fpend) and the urbanization waterproofed area (AIUrb). The methodology by which the AIUrb variable was defined did not incorporate low-density urban land use areas since high percentages of anthropization of the soil were included for the waterproofed area. This means that, despite the anthropization of natural areas, low-density areas offer large areas to absorb excess rainfall.

The result was 6 raster images (Fig. 4) where the values were associated with a table from 0 to 1. Where zero was the pixel with the least capacity to influence the model and 1 was associated with the maximum biomass values, the area impermeabilized by urbanization, the greatest amount of precipitation received, the best infiltration capacity, and in the case of the slope this relationship was inverse, considering the greater the slope the lower the retention capacity.

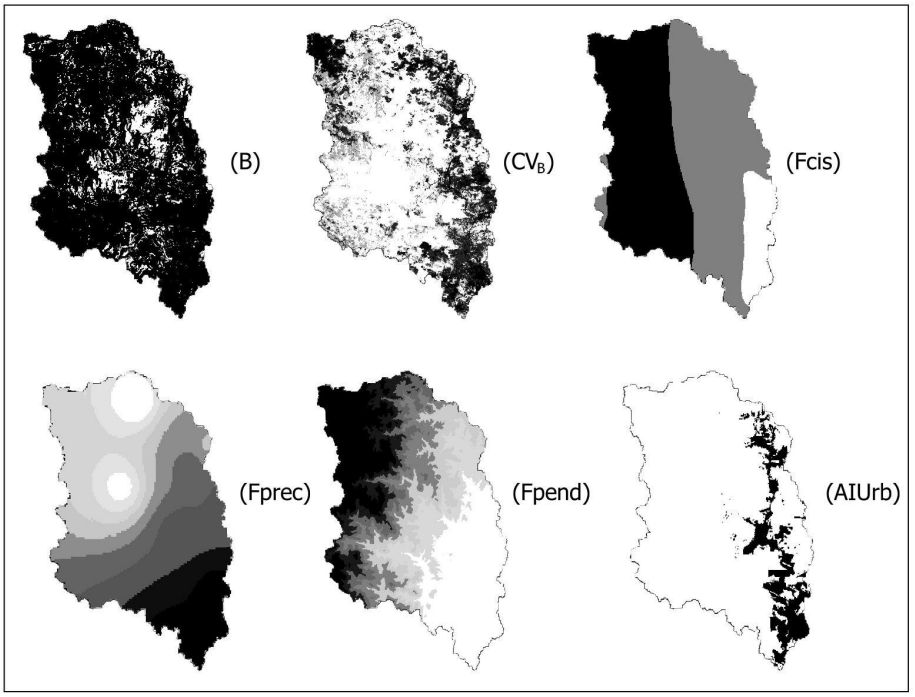

Figure 4. Intermediate products:. Biomass (B), biomass stability (CV_B), soil infiltration capacity (Fcis), Precipitations (Fprec), Slope (Fpend), urbanization waterproofed area (AIUrb).

3.2. *The REP model for environmental buffer areas*

REP values were obtained for the northwest catchment area of the AMC. These range from -0.001 located in areas of intermediate slope but poor vegetation coverage and, the maximum values up to 0.79. In a first observation, the highest values are associated with areas of biomass concentration, in zones of intermediate slope (in the catchment), and with high proximity to the urbanization of the valley (Figure 5).

It was deduced that in the catchment outflow area, the percentage of impermeabilization was high, which means low levels of retention. This was already observed in the building of the AIUrb layer because the pixel is mainly urban and the average block belongs more to the Córdoba city than to the mountain valley.

In the first instance, the close relationship between the exposure of human settlements (both in the serrano valley and those near the city of Córdoba), during the occurrence of extraordinary rainfall events for the sector, was observed. This is associated to the low capacity of the area to retain rainfall excesses, the slope and the decisive influence of the urban area on the values of the indicator.

In addition, it was inferred that the areas with greater capacity to retain excess rainfall correspond to the mean values of slope and greater areas of forest concentration. Based on specific literature, these values correspond to areas of mountain forest and piedmont forest (Gavier and Bucher, 2004). However, in recent years the Sierras Chicas sector has shown a strong presence of exotic species (mainly ligustrum lucidus forests) (Zeballos et al., 2014). Given the proportion of these species it is possible to estimate their presence in the basin.

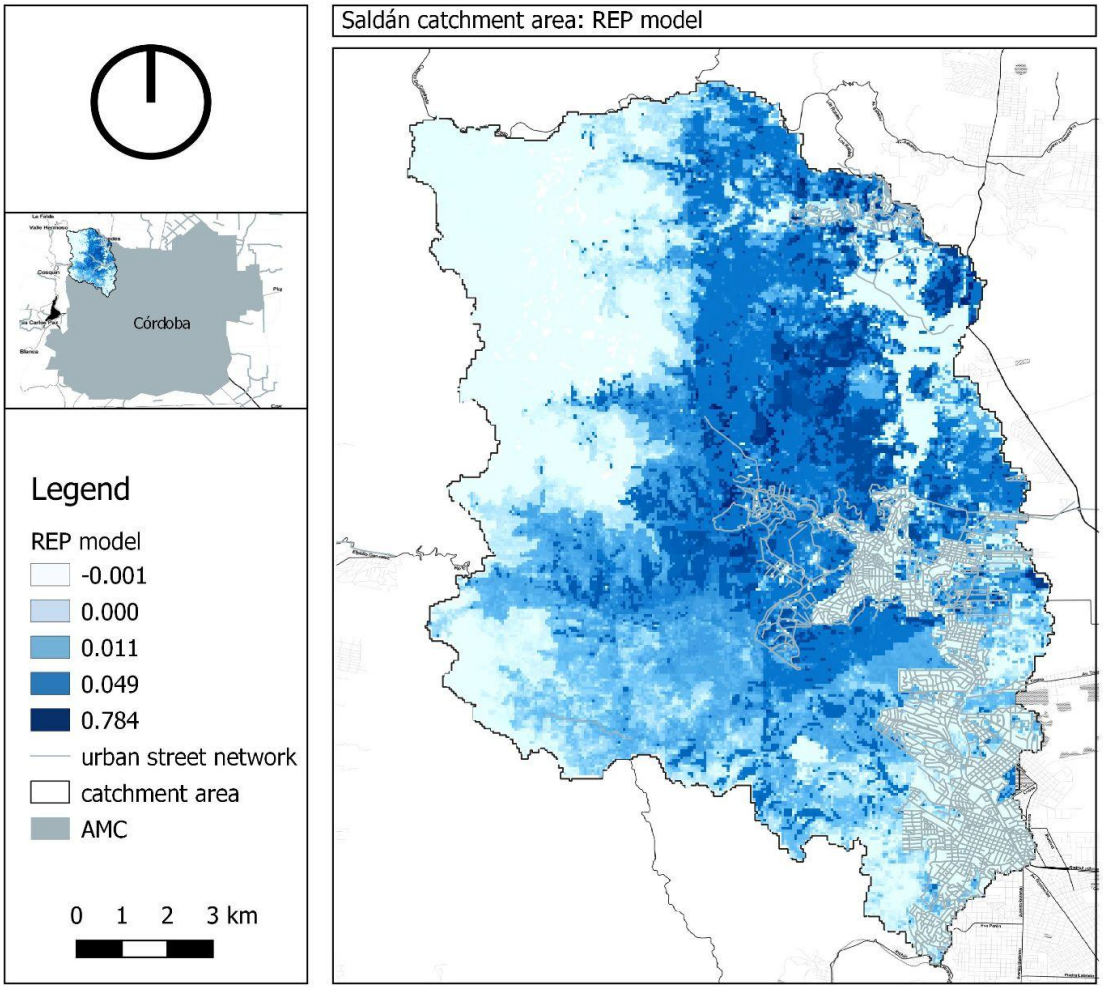

Figure 5. Retention of excess precipitation by vegetation index (REP) for urban-natural interface in Saldán basin area.

3.3. Validation model

The spectral response of the band ratio proposed by the LSWI allowed discriminating values of water presence in the soil without the need for additional calculations. In order to discriminate between dry and wet periods within the year analyzed, monthly precipitation values for 3 points of the area were taken from the open data of the National Ministry of Agriculture, Livestock and Fisheries (2022) (Table 1). From the location and processing of available data, 3 groups of data or periods were formed. A dry period: from May to September and two wet periods: January-April and October-December, from these data the stacks of temporal derivatives of LSWI were made.

	Mean precipitation (mm)		
GPS point	(-64.508, -31.306)	(-64.273, -31.449)	(-64.316, -31.159)
January	128	134	134
February	128	129	129

March	131	130	130
April	68	65	65
May	20	22	22
June	6	9	9
July	16	23	23
August	6	7	7
September	30	32	32
October	71	70	70
November	107	108	108
December	126	129	129

Table 1. Precipitaciones mensuales-cuenca Saldán. Se diferenciaron 3 períodos dentro del año: Enero-Abril, Mayo-Septiembre y Octubre-Diciembre. Fuente: ex Ministerio de Agroindustria: datos abiertos. Precipitaciones mensuales TRMM https://geoportal.agroindustria.gob.ar/sirmin/clima.html

The variation of soil moisture was analyzed and the results of the dry-wet period were compared (Fig. 6). In the pairs of scenes of wet period 1, no stable presence of water in the soil was observed. Since this period is also the one with the highest annual rainfall (Table 1), the data are compared with the dry period where the pixels that show no variation between pairs of analyzed scenes are considerably fewer and are concentrated in the middle area of the basin, associated with the area of vegetation cover with the highest biomass values observed in the intermediate products. Wet period 2 was observed as intermediate between the first and the dry period, since it presents a greater number of pixels with good retention than the dry period, but fewer than the first one.

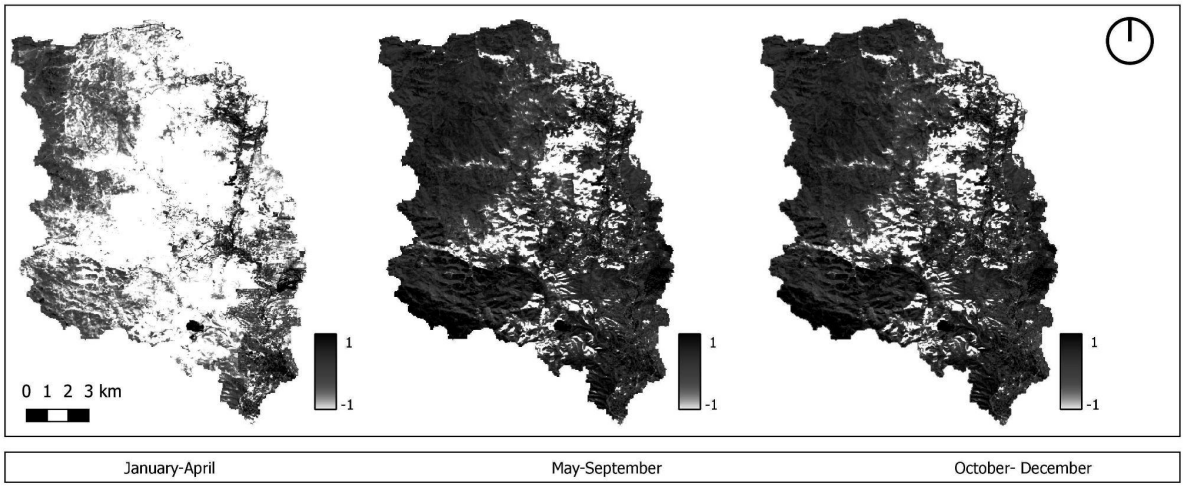

Figure 6. Soil moisture loss in the catchment. Wet and dry periods year 2017. Pixel values closer to 0 are inferred as those with less variation in soil moisture presence between pairs of calculated scenes.

3.4. Ecosystem protection areas in urban catchments

The maximum values (1209 ha) of excess precipitation retention by vegetation cover (REP) were compared with the spatial location of those pixels with lower soil moisture loss from the temporal variation rate of LSWI (1875 ha). Of the total of both models calculated (Fig. 7), a spatial coincidence of 900 ha was verified. This determines that there is a margin of error of 39% of pixel assignment of which may or may not be retention pixels. However, the inputs that fed each model are relevant in the construction of a synthetic function of ecosystem processes in the basin. Given that the validation model identified a greater number of soil moisture retention areas, it is expected that the variables associated with slope, biomass specificity and its variation, as well as soil characteristics and impervious area, establish incidence weights that respond to local data but help to better delimit a specific model.

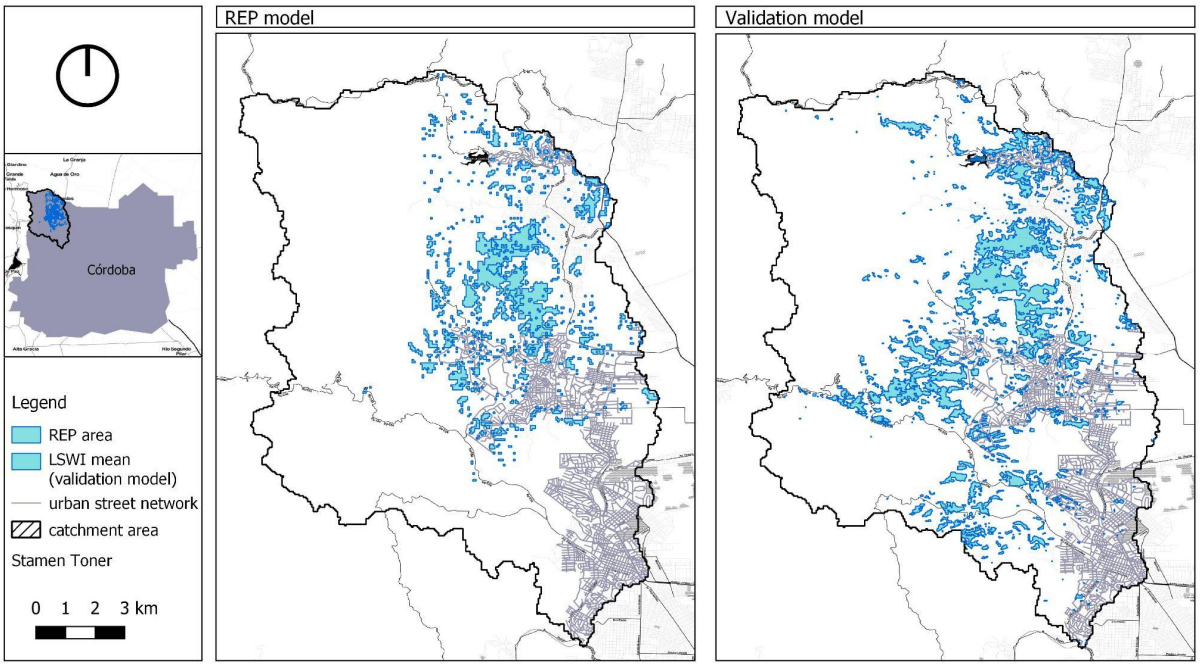

Figure 7. Retention of excess rainfall by vegetation cover (left) REP model, (right) Mean LSWI derivative.

3.5. Final considerations

The REP index was studied, modified and proposed as an input to rethink the way in which the territory is planned and to point out that fundamental processes - such as those of water, forest or soil - can be critical if they are urbanized without assessing the impact, not only in terms of people's lives - when floods occur - but also of the goods that are lost due to the occurrence of extraordinary events. It is also essential to make visible processes that are not taken into account in local and regional planning.

The spatialization of these results is based on a relationship of variables involved with water retention and although it is used as an indicator, the way in which these variables are related could be approached with a higher level of complexity, assigning different weights and thus establishing the implication of the different parameters in the final model. Although model assumptions could be validated, it is necessary to have field truth at the basin scale at the immediate time of the event studied.

The validation stage established a type of accuracy of the model representation for the system studied, with the objective of justifying that the REP model, within its applicability domain, has a satisfactory range of accuracy consistent with the intended application. Although the validity is associated with the specific purpose of configuring a basis of analysis of ecosystem protection areas at the basin scale, the need for local work, where there is the possibility of post-event validation, is reinforced.

The contribution of ecosystems, and especially of the uses and transformations to which they are subjected by the different processes of anthropization, and in this particular case on the hydrological cycle, shows systematic relations at different scales of the LUP and involves, in the same way, different political decision-makers. There is no point in a locality defining zones of maximum ecosystem protection and the neighboring city developing or waterproofing areas of the basin headwaters.

4. Acknowledgments

This work is part of a doctoral fellowship from the National Council of Scientific and Technical Research -CONICET- without which it would not have been done. We thank all the experts and researchers of the National Institute of Agricultural Technology -INTA- who have participated directly and indirectly in this work. To the ECO-SER team and in particular to Paula Barral who was consulted when this process began and Verónica Bustos, from Soil Map Plan -EEA Manfredi-. This research began to be done in the framework of the National Program of Natural Resources, environmental management and Ecoregions that was part of INTA's program portfolio between 2014 and 2018. It was concluded in the framework of INTA's Structural Projects: Socio-Agro-Environmental Alternatives: Prospective, Observatories and Land Management for Agrifood Sustainability (PEI205) and Prevention and Evaluation of Agricultural Emergencies and Disasters (PEI064).

5. References

Arias, G. C. and Campana, H. O. (2012) 'Ley 9841. Regulación de los usos del suelo en la región metropolitana de Córdoba. Sector primera etapa', *Legislatura de la provincia de Córdoba*.

Ambrosino, Silvio et al. 2004. *Inundaciones urbanas en Argentina*. 1ra ed. ed. Juan Carlos Bertoni. Córdoba: Estudio Tríptico.

Bahill, J. *et al.* (2015) *Recursos Naturales de la Provincia de Córdoba. LOS SUELOS. Nivel de Reconocimiento 1:500.000*, *GeoINTA*. Available at: http://www.geointa.inta.gob.ar/2015/01/29/suelos-de-cordoba-1500-000/ (Accessed: 25 April 2018).

Barral, M. P. (2016) *Tutorial mapeo ECOSER. Protocolo colaborativo de evaluación y mapeo de servicios ecosistémicos y vulnerabilidad socio-ecológica para el ordenamiento territorial*. versión actualizada a diciembre 2016. Buenos Aires.

Barchuk, Alicia. 2016. *Riesgos En Sierras Chicas Ante Los Cambios de Uso Del Suelo.* Tecyt. Taller de estudios de la ciudad y el territorio (2): 26–31. https://revistas.unc.edu.ar/index.php/tecyt/article/view/15293.

Carreño, L., Frank, F. . and Viglizzo, E. . (2012) 'Agriculture , Ecosystems and Environment Tradeoffs between economic and ecosystem services in Argentina during 50 years of land-use change', *Agriculture, Ecosystems and Environment*, 154, pp. 68–77. doi: 10.1016/j.agee.2011.05.019.

Carreño, L. and Viglizzo, E. (2007) *Provisión de servicios ecológicos y gestión de los ambientes rurales en Argentina*. Buenos Aires: INTA Ediciones.

Ceccato, P., Flasse, S. and Grégoire, J.-M. (2002) 'Designing a spectral index to estimate vegetation water content from remote sensing data Part 2 . Validation and applications', *Remote Sensing of Environment*, 82, pp. 198–207.

Céliz, Y., & Maidana, C. E. (2019). *Transformaciones ambientales en interfases antrópicas: análisis del área metropolitana de Córdoba a través de Google Earth Engine*. In XI Congreso de AgroInformática (CAI)-JAIIO 48 (Salta, 2019).

Céliz, Y. (2020). *Una construcción compleja de la interfase territorial. Revisión conceptual para la generación de variables de análisis*. Papeles de Geografía, (66).

Chandrasekar, K., Sai, M. V. R. S. and Roy, P. S. (2010) 'Land Surface Water Index (LSWI) response to rainfall and NDVI using the MODIS Vegetation Index product', *International Journal of Remote Sensing*, 31(15), pp. 3987–4005. doi: 10.1080/01431160802575653.

COTBN (2009) *Proyecto de ley de ordenamiento territorial de bosques nativos de la provincia de Córdoba*, *Programa de Ordenamiento Territorial de los Bosques Nativos de la provincia de Córdoba*. Córdoba.

GAO, B.C., 1996, *NDWI – a normalized difference water index for remote sensing of vegetation liquid water from space*. Remote Sensing of Environment, 58, pp. 257–266.

García Peyrano, R. (2011) *Lineamientos del Plan estratégico urbano territorial del área metropolitana de Córdoba. Definición del plan vial y uso del suelo*. Córdoba.

Gavier, G. I. and Bucher, E. H. (2004) 'Deforestación de las sierras chicas de Córdoba (Argentina) en el período 1970-1997', *Academina Nacional de Ciencias. MIscelánea*, 101, pp. 4–27.

Gerberman, A. J., Cuellar, J. A. and Gausman, H. W. (1984) 'Relationship of sorghum canopy variables to reflected infrared radiation for 2 wavelengths and 2 wavebands', *Photogrammetric Engineering & Remote Sensing*, (50), pp. 209–214.

Gianre, L. (2015) 'El informe científico de la UNC que explica las inundaciones en las Sierras Chicas de Córdoba', *UNCiencia*, 18 March, pp. 1–5. Available at: http://www.unciencia.unc.edu.ar/2015/marzo/el-informe-cientifico-de-la-unc-que-explica-las-inundaciones-en-las-sierras-chicas-de-cordoba.

Giobellina B. (2016) *La problemática de los entornos rurales. El caso del cinturón verde de Córdoba.* pp. 14-19. Tecyt (2). Facultad de Arquitectura, Urbanismo y Diseño, Universidad Nacional de Córdoba. ISSN: 2525-1031.

Giobellina, B. L., Marinelli, M. V., Lobos, D. A., Eandi, M., Bisio, C., Butinof, M., ... Romero Asis, M. (2022). *Producción frutihortícola en la Región Alimentaria de Córdoba. Caracterización y mapeo 2018-2020*. Ediciones INTA; Agencia de Extensión Rural Córdoba.

Gorelick, N. *et al.* (2017) 'Google Earth Engine : Planetary-scale geospatial analysis for everyone', *Remote Sensing of Environment*. The Author(s), 202, pp. 18–27. doi: 10.1016/j.rse.2017.06.031.

de Groot, R. S. *et al.* (2010) 'Challenges in integrating the concept of ecosystem services and values in landscape planning, management and decision making', *Ecological Complexity*. Elsevier B.V., 7(3), pp. 260–272. doi: 10.1016/j.ecocom.2009.10.006.

Haines-Young, R. and Potschin, M. (2010) 'The links between biodiversity , ecosystem services and human well-being', in Raffaelo, D. G. and Frid, C. J. J. (eds) *Ecosystem Ecology: A New Synthesis*. Cambridge University Press.

Instituto Nacional del Agua-Centro de Región Semiárida INA-CIRSA (2004) *Inundaciones repentinas en las sierras de Córdoba*. Primeras jornadas de debate sobre riesgo hídrico, inundaciones y catástrofes, Buenos Aires.

Jackson, T. J. *et al.* (2004) 'Vegetation water content mapping using Landsat data derived normalized difference water index for corn and soybeans', 92, pp. 475–482. doi: 10.1016/j.rse.2003.10.021.

Jobbágy, E. G. (2011). *Servicios hídricos de los ecosistemas y su relación con el uso de la tierra en la llanura chaco-pampeana.*. In Valoración de Servicios Ecosistémicos Conceptos, herramientas y aplicaciones para el ordenamiento territorial. Ediciones INTA, 163-183.

Jürgens, C. (1997) 'The modified normalization difference vegetation index (mNDVI): a new index to

determine frost damages in agriculture based on Landsat TM data', *International Journal of Remote Sensing*, (18), pp. 3583–3594.

Justice, C. O. *et al.* (1985) 'Analysis of the phenology of global vegetation using meteorological satellite data', *International Journal of Remote Sensing*, 6(8), pp. 1271–1318.

Laterra, P. *et al.* (2015) 'ECOSER: Protocolo colaborativo de evaluación y mapeo de servicios ecosistémicos y vulnerabilidad socio-ecológica para el ordenamiento territorial', p 58. Available at: http://eco-ser.com.ar/.

Laterra, P. and Nahuelhual, L. (2015) 'Internalización de los servicios ecosistémicos en el ordenamiento territorial rural: bases conceptuales y metodológicas', in Paruelo, J. M. et al. (eds) *Ordenamiento territorial rural. Conceptos, métodos y experiencias*. FAO-MINAGRI-FAUBA, pp. 86–106. Available at: http://www.fao.org/3/a-i4195s.pdf.

Lehmann, G. (2015) 'Sierras Chicas: muerte, desastre y destrucción por las lluvias', *La Voz del interior*, February. Available at: https://www.lavoz.com.ar/ciudadanos/sierras-chicas-muerte-desastre-y-destruccion-por-las-lluvias.

Mitas, L. and Mitasova, H. (1999) 'Spatial interpolation', in *Geographical Information Systems: Principles, Techniques, Applications, and Management*, pp. 481–492.

Moeslund, J. E. *et al.* (2013) 'Topography as a driver of local terrestrial vascular plant diversity patterns Special Invited Review', *Nordic Journal of Botany*, 31(January), pp. 129–144. doi: 10.1111/j.1756-1051.2013.00082.x.

Paruelo, J. M. (2008) 'La caracterización funcional de ecosistemas mediante sensores remotos', *Ecosistemas*, 17(3), pp. 4–22.

Postel, S. L. and Thompson, B. H. (2005) 'Watershed protection: Capturing the benefits of nature's water supply services', *Natural Resources Forum*, 29(2), pp. 98–108. doi: 10.1111/j.1477-8947.2005.00119.x.

QGIS Development Team (2016) 'QGIS geographic information system. Open source geospatial fundation project'.

Raudsepp-Hearne, C., Peterson, G. D., & Bennett, E. M. (2010). *Ecosystem service bundles for analyzing tradeoffs in diverse landscapes*. Proceedings of the National Academy of Sciences, 107(11), 5242-5247.

Ross, E. *et al.* (2019) 'Large-scale probabilistic identification of boreal peatlands using Google Earth Engine , open-access satellite data , and machine learning', pp. 1–23.

Sellers, P. J. (1985) 'Canopy reflectance , photosynthesis and transpiration', *International Journal of Remote Sensing*, 6(8), pp. 1335–1372.

Tucker, C. J. (1977) 'Resolution of grass canopy biomass classes', *Photogrammetric Engineering & Remote Sensing*, (43), pp. 1059–1067.

Tucker, C. J. (1979) 'Red and photographic infrared linear combinations for monitoring vegetation', *Remote Sensing of Environment*, (8), pp. 127–150.

Waqar, M. M., Mirza, J. F., Mumtaz, R., & Hussain, E. (2012). Development of new indices for extraction of built-up area & bare soil from landsat data. Open Access Scientific Reports, 1(1), 4.

Xiao, X Boles, S Frolking, S. *et al.* (2002) 'Observation of flooding and rice transplanting of paddy rice fields at the site to landscape scales in China using VEGETATION sensor data', *International Journal of Remote Senging*, (82), pp. 3009–3022. doi: 10.1080/01431160110107734.

Xiao, X. *et al.* (2004) 'Modeling gross primary production of temperate deciduous broadleaf forest using satellite images and climate data', *Remote Sensing of Environment*, 91, pp. 256–270. doi: 10.1016/j.rse.2004.03.010.

Zeballos, S. R. *et al.* (2014) 'Composición de especies leñosas en comunidades invadidas en montañas del centro de Argentina : su relación con factores ambientales locales', *Revista de Biología Tropical*, 62(4), pp. 1549–1563.